PERGAMON

Atmospheric Environment 33 (1999) 745–757

ATMOSPHERIC ENVIRONMENT

Prediction of multicomponent inorganic atmospheric aerosol behavior

Asif S. Ansari, Spyros N. Pandis*

Departments of Chemical Engineering and Engineering and Public Policy, Carnegie Mellon University, 5000 Forbes Ave., Pittsburgh, PA 15213, USA

Received 13 January 1998; accepted 8 June 1998

Abstract

Many existing models calculate the composition of the atmospheric aerosol system by solving a set of algebraic equations based on reversible reactions derived from thermodynamic equilibrium. Some models rely on an a priori knowledge of the presence of components in certain relative humidity regimes, and often fail to accurately predict deliquescence point depression and multistage aerosol growth. The present approach, relying on adjusted thermodynamic parameters of solid salts and a state of the art activity coefficient model, directly minimizes the Gibbs free energy (according to thermodynamic equilibrium principles) given temperature, relative humidity and the total (gas plus aerosol) ammonia, nitric acid, sulfate, sodium, and hydrochloric acid concentrations. A direct minimization, while requiring no additional assumptions in its algorithm, allows the elimination of many of the assumptions used in previous models such as divided relative humidity (rh) and composition domains where only certain reactions are assumed to occur and constant DRH values despite varying temperature and composition. Moreover, the current approach predicts aerosol deliquescence and efflorescence behavior explaining the existence of supersaturated aerosol solutions. A comparison is conducted between our approach and available experimental results under several conditions. The current model agrees with experimental results for single salt systems although it shows sensitivity to thermodynamic parameters used in the minimization algorithm. A set of ΔG_f^0 for solid salts is estimated that is consistent with available laboratory measurements and significantly improves model performance. For multicomponent systems, the current approach with adjusted ΔG_f^0 accurately reproduces observed multistage growth patterns and deliquescence point depression over a broad temperature range. Finally, the direct Gibbs free energy minimization accurately reproduces aerosol efflorescence behavior.

Keywords: Gibbs free energy minimization; Deliquescence; Efflorescence; Inorganic aerosols; Thermodynamic equilibrium

1. Introduction

Aerosols are known to have a significant role in the atmosphere having adverse impacts on human health and directly affecting air quality, visibility, and climate change. To better understand such processes, accurate methods in predicting atmospheric aerosol composition are essential. One of the most challenging tasks for the available models is the prediction of the partitioning of the volatile inorganic aerosol components (ammonia, nitric acid, water, etc.) between the gas and aerosol phases.

*Corresponding author.

1352-2310/99/$ – see front matter
PII: S1352-2310(98)00221-0

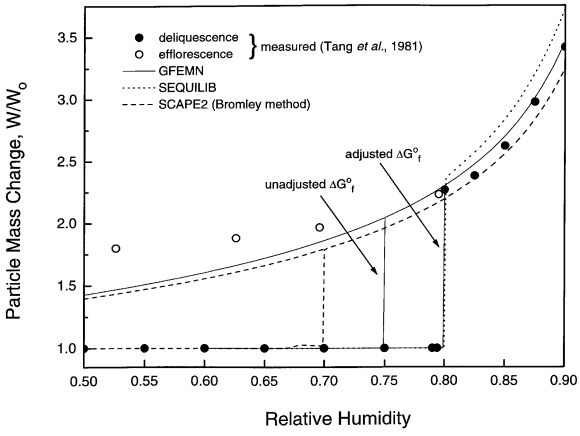

Fig. 1. Particle mass change at 25°C for an $(NH_4)_2SO_4$ particle as a function of relative humidity: model prediction versus observed results (Note: since SCAPE2 allows computation with any of the three mentioned multicomponent activity coefficient methods, that returning the best results is used and noted for SCAPE2).

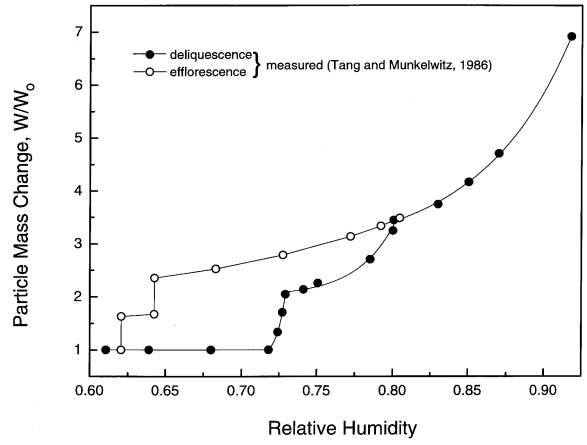

Fig. 2. Measured particle mass change at 25°C for a mixed salt particle (initially 66 wt% KCl, 34 wt% NaCl) as a function of relative humidity.

Ammonia, sulfate, nitrate, sodium, and chloride are the dominant reactive inorganic aerosol components in the atmosphere. Aerosols can exist in the form of solids such as NH_4NO_3 or $(NH_4)_2SO_4$ and aqueous solutions of electrolytes such as NH_4^+, SO_4^{2-}, and NO_3^- (Wexler and Seinfeld, 1991). Fig. 1 shows the typical behavior of an $(NH_4)_2SO_4$ particle as a function of relative humidity (rh). As the rh increases, the particle remains dry until it suddenly absorbs water increasing in size at 80% rh. The rh at which the solid to liquid-phase transition occurs is referred to as the deliquescence relative humidity (DRH); the growth pattern exhibited by an aerosol during increasing rh is known as deliquescence. However, the $(NH_4)_2SO_4$ particle follows a different path (efflorescence path) during decreasing rh. Instead of crystallizing at its DRH, the aerosol follows the thermodynamically less favorable path by becoming a supersaturated solution until a much lower rh (30% rh for $(NH_4)_2SO_4$) at which crystallization eventually occurs. This "hysteresis" behavior exhibited by atmospheric aerosols has been observed in a number of studies (Tang et al., 1977; Hanel and Lehmann, 1981; Winkler, 1986). The crystallization point of particles can be determined experimentally, and sometimes cannot be reproduced reliably because of high sensitivity to trace impurities (Tang et al., 1977).

The behavior of aerosols becomes increasingly complex as more components are added to the system. The behavior of a mixed NaCl–KCl particle in Fig. 2 (Tang and Munkelwitz, 1986) indicates that systems of higher complexity exhibit multistage deliquescence and efflorescence patterns. As single salts, NaCl and KCl deliquesce at 75.3 and 84.2% rh respectively at 25°C, yet according to the measured growth profile of Fig. 2, the DRH of the NaCl–KCl particle is 72%. Wexler and Seinfeld (1991) have shown that the DRH of a multicomponent particle is lower than that of its components. Depending on the rh and composition of a multicomponent system, an aerosol particle may contain both a solid and aqueous phase with each phase containing a combination of components. The NaCl–KCl system exhibits a hysteresis behavior with two distinct crystallization points as rh decreases. Thus, the difficulty in predicting the composition of aerosols is a result of their ability to consist of more than one phase and to exhibit deliquescence or efflorescence behavior depending on the history of the rh.

Over the past 15 years, several aerosol models have been developed relying on thermodynamic equilibrium principles to predict the composition and physical state of inorganic atmospheric aerosols. It has been widely assumed that volatile species in the gas and aerosol phases are in chemical equilibrium (Stelson and Seinfeld, 1982a, b; Bassett and Seinfeld, 1983; Saxena et al., 1986; Pilinis and Seinfeld, 1987). Previous work by Hildemann et al. (1984) has confirmed the general agreement of ambient inorganic aerosol measurements with those predicted by thermodynamic equilibrium. However, in cases where the equilibrium timescale is long relative to the residence time of particles in a given environment, thermodynamic equilibrium may not be a good approximation (Wexler and Seinfeld, 1990; Meng and Seinfeld, 1996). Aerosol models based on thermodynamic equilibrium include EQUIL (Bassett and Seinfeld, 1983), MARS (Saxena et al., 1986), SEQUILIB (Pilinis and Seinfeld, 1987), AIM (Wexler and Seinfeld, 1991), SCAPE (Kim et al., 1993a), SCAPE2 (Meng et al., 1995) and EQUISOLV (Jacobson et al., 1996). These models have been developed for atmospheric simulations and thus, computational efficiency was a major objective during

their development. To attain high computational efficiency, assumptions were made to simplify the problem at hand and allow use of the equilibrium models in Eulerian atmospheric chemical transport models. Three-dimensional models capable of tracking aerosol dynamics (transport of gases to particles, particle formation, and size distribution) have been combined with SEQUILIB (Pilinis and Seinfeld, 1988; Lurmann et al., 1997) and EQUISOLV (Jacobson et al., 1996) to simulate the behavior of organic and inorganic aerosols. Although limited comparisons among equilibrium models have been conducted (Wexler and Seinfeld, 1991; Kim et al., 1993b), no detailed comparison to observations of aerosol behavior has been performed in part due to limited availability of such measurements; the ability to reproduce laboratory aerosol observations is yet unknown. The equilibrium models mentioned may agree with each other within a 5–10% error, but if they cannot reproduce observed aerosol behavior, their results may introduce errors in atmospheric simulations. Is it possible to reproduce complex growth patterns in light of what has been observed for multicomponent systems? In an attempt to answer this question, a model predicting inorganic aerosol composition and state is developed without concern for computational efficiency. Our main objective is to evaluate our current ability to model aerosol behavior. The model directly minimizes the total Gibbs free energy of the aerosol system of interest with adjusted thermodynamic parameters for solid salts and the activity coefficient model of Clegg et al. (1998). An analysis of the energy minimization approach is given and its predictions compared with those of other models and with experimental observations are examined.

2. Thermodynamics of aerosols

For a closed system, the Gibbs free energy (G) at constant temperature and pressure is (Denbigh, 1981):

$$G = \sum_i n_i \mu_i \tag{1}$$

where n_i is the concentration of component i (mol m^{-3}) and μ_i is its chemical potential (kJ mol^{-1}). Denbigh also shows that for such a system at equilibrium, G will be at its minimum possible value. Since atmospheric systems consist of gases, liquids, and solids, each phase must be accounted for in Eq. (1). The chemical potential μ_i is defined for liquid solutions, ideal gases, and solids, respectively, as

$$\mu_i = \mu_i^0(T) + RT \ln(\gamma_i m_i) \tag{2}$$

$$\mu_i = \mu_i^0(T) + RT \ln(p_i) \tag{3}$$

$$\mu_i = \mu_i^0(T) \tag{4}$$

where R is the gas constant (0.0083145 kJ mol^{-1}), T is the temperature (K), $\mu_i^0(T)$ is the standard chemical potential (kJ mol^{-1}), γ_i is the mean activity coefficient, m_i is the molality (mol kg^{-1} water), and p_i is the partial pressure (atm) of component i. The standard chemical potential $\mu_i^0(T)$, can be determined from:

$$\mu_i^0(T) = T\left[\frac{\Delta G_f^0}{T_o} + \Delta H_f^0\left(\frac{1}{T} - \frac{1}{T_0}\right) + c_p\left(\ln\frac{T_o}{T} - \frac{T_o}{T} + 1\right)\right] \tag{5}$$

where ΔG_f^0 is the free energy of formation (kJ mol^{-1}), ΔH_f^0 is the standard heat of formation (kJ mol^{-1}), and c_p is the heat capacity (kJ mol^{-1} K^{-1}), all at T_o, a reference temperature (K) usually taken as 298.15 K. Wagman et al. (1982) have compiled data for ΔG_f^0, ΔH_f^0, and c_p for an extensive number of species of atmospheric importance (Table 1).

To determine γ_i in a multicomponent solution, many different approaches have been used including methods by Bromley (1973), Kusik and Meissner (KM, 1978), and Pitzer (1986). Clegg and Brimblecombe (1995) however, noted that for atmospheric applications, these previous activity coefficient methods, although simple, are sometimes inaccurate in modeling atmospheric aerosols, especially at conditions close to saturation and at supersaturation. Clegg and Pitzer (1992a, b) and Clegg et al. (1994) developed a new activity coefficient model applicable to multicomponent solutions based on an extended form of Pitzer's method. It has been applied to several systems and can accurately predict solute ion activities (Clegg and Brimblecombe, 1994, 1995; Clegg et al., 1996). Recently, Clegg et al. (1998) extended their method to include H^+, NH_4^+, Na^+, NO_3^-, HSO_4^-, SO_4^{2-}, and Cl^- at 25°C. Since this model has been shown to be accurate to within experimental error at conditions including low rh and high supersaturation for certain systems, we use it for determining γ_i in Eq. (2).

Applying phase equilibrium to water, it can be shown that the activity of water (a_w) is equal to the rh in the atmosphere. Given a_w and the concentrations of aqueous components, the water content (W, kg m^{-3} air) of a multicomponent solution can be determined by the ZSR method (Chen et al., 1973):

$$W = \sum \frac{M_i}{m_{io}(a_w)} \tag{6}$$

where M_i is the molar concentration of electrolyte i (mol m^{-3} air), and $m_{io}(a_w)$ is the molality of a single component aqueous solution of electrolyte i with a_w = rh. Electrolyte molalities over a range of a_w for species of atmospheric interest are available in Cohen et al. (1987), Chan et al. (1992), and Tang and Munkelwitz (1994a). Although alternate methods exist

Table 1
Thermodynamic properties for atmospheric aerosol species

Species	ΔG_f^0 (kJ mol^{-1})	ΔH_f^0 (kJ mol^{-1})	C_p^0 (J mol^{-1}-K)	Adj. ΔG_f^0 (kJ mol^{-1})	% Deviation	DRH[d]
NH_4NO_3(s)	− 183.87	− 365.56	139.30	− 184.55	0.37	0.62
$(NH_4)_2SO_4$(s)	− 901.67	− 1180.85	187.49	− 903.15	0.16	0.80
NH_4HSO_4(s)	− 823.00[b]	− 1026.96	127.50[a]	− 822.80	0.02	0.40
$(NH_4)_3H(SO_4)_2$(s)	− 1730.00[b]	− 2207.00[b]	315.00[a]	− 1733.07	0.18	0.69
Na_2SO_4(s)	− 1270.16	− 1387.08	128.20	− 1269.52	0.05	0.84
$NaHSO_4$(s)	− 992.80	− 1125.50	85.00[a]	− 1005.27	1.26	0.52
NaCl(s)	− 384.14	− 411.15	50.50	− 384.48	0.09	0.75
$NaNO_3$(s)	− 367.00	− 461.75[e]	92.88	− 367.12	0.03	0.74
NH_4Cl(s)	− 202.87	− 314.43	84.10	− 204.79	0.95	0.80
NH_3(g)	− 16.45	− 46.11	35.06			
HNO_3(g)	− 74.72	− 135.06	53.35			
HCl(g)	− 95.30	− 92.31	29.13			
H_2O(g)	− 228.57	− 241.82	33.58			
H_2O(l)	− 237.13	− 285.83	75.29			
NH_4^+(aq)	− 79.31	− 132.51	79.90			
Na^+(aq)	− 261.91	− 240.12	46.40			
NO_3^-(aq)	− 111.25	− 207.36	− 86.60			
SO_4^{2-}(aq)	− 744.53	− 909.27	− 293.00			
Cl^-(aq)	− 131.23	− 167.16	− 136.40			
HSO_4^-(aq)	− 755.91	− 887.34	− 84.00			

All values are from Wagman et al. (1982) unless otherwise noted.
[a]Wexler and Seinfeld (1991).
[b]Basset and Seinfeld (1983).
[c]HNO_3(aq) is listed instead since that from Wagman is in error.
[d]Pilinis and Pandis (1995).
[e]Adjusted value (1.3% deviation) is listed instead based on measurements of temperature dependence of DRH.

for determining the water content of electrolyte systems, the ZSR method agrees with experimental data up to high ionic strengths and is computationally efficient. Electrolyte molalities can be calculated after the water content has been determined thus allowing the calculation of γ_i.

3. Model formulation

3.1. Direct minimization of Gibbs free energy

The atmospheric system of interest includes the following components:

gas phase: NH_3, HNO_3, HCl, H_2O
aerosol liquid phase: H^+, NH_4^+, Na^+, Cl^-, NO_3^-, HSO_4^-, SO_4^{2-}, H_2O
aerosol solid phase: $(NH_4)_2SO_4$, NH_4HSO_4, $(NH_4)_3H(SO_4)_2$, NH_4NO_3, NH_4Cl, Na_2SO_4, $NaHSO_4$, $NaNO_3$, NaCl.

Since sulfuric acid has a very low vapor pressure at ambient rh, it can be assumed that all sulfate lies in the aerosol phase. Therefore, all sulfate containing components are either solid and/or liquid at any given time with the amounts in each phase governed by thermodynamic equilibrium. Double salts such as hydrates and decahydrates of solid components are not included; their exclusion will be discussed in a later section. For a given temperature, pressure, rh, total ammonia (TA), nitrate (TN), sodium (TD), chloride (TC), and sulfate (TS) concentrations, the problem to be solved based on (1) is

$$\begin{aligned} &\text{Min } G = \sum_i n_i \mu_i \\ &\text{s.t. } \sum_a v_a n_a - \sum_c v_c n_c = 0 \\ &\sum_i \omega_i n_i = \text{TA} \\ &\sum_i \omega_i n_i = \text{TN} \\ &\sum_i \omega_i n_i = \text{TD} \\ &\sum_i \omega_i n_i = \text{TC} \\ &\sum_i \omega_i n_i = \text{TS} \end{aligned} \tag{7}$$

where v is the ion charge, ω is the stoichiometric coefficient of a component in species i (i.e. 2 for ammonium in $(NH_4)_2SO_4$, 1 in NH_4^+, etc.) and subscripts are as follows:

i all components
a all anions
c all cations.

The first constraint corresponds to the electroneutrality balance whereas the latter five constraints correspond to conservation of mass.

The potential solution space of the partitioning problem is bounded for each species for each phase (gas, solid particulate, and aqueous particulate) by zero and the total concentration of the species. For example, the concentration of aqueous aerosol nitrate will be equal or greater than zero and equal or less than the total nitrate concentration, TN. This space is further limited by the electroneutrality and mass balance constraints shown in Eq. (7). Our algorithm first determines the allowable solution space. This solution space that satisfies all the constraints is then searched and G of each composition is determined using a relatively coarse resolution. A first guess of the minimum G is determined this way. The resolution of the search is then increased around the area of the first guess and a solution with the desired accuracy is determined; the search continues until a specified degree of accuracy is obtained. Upon completing the search, the algorithm returns both gas and aerosol concentrations corresponding to the minimum G.

This exhaustive search approach is feasible because the solution space is easily determined. This is not the case for the problem of calculating the equilibrium concentrations of particles of a given composition, for example AIM (Wexler and Seinfeld, 1991). In that case the solution space is theoretically semi-infinite and other methods must be used for the determination of the minimum G.

Since Eq. (7) is a minimization problem, there are many sets of variables n_i that satisfy all the constraints with only one set globally minimizing G, the stable equilibrium condition of the system. Local minima of G satisfying the constraints correspond to metastable equilibrium points. The minimization algorithm shown in Eq. (7) is similar to that first used in the atmospheric aerosol equilibrium model EQUIL of Bassett and Seinfeld (1983). EQUIL incorporates the extents of reaction, ξ, into the minimization, and is therefore based on a given set of reactions assumed to occur. Our proposed formulation, Eq. (7), does not explicitly depend on a given set of reactions.

With Eq. (7), the DRH of any aerosol system can be determined. Consider a single particle which can exist as a solid, liquid, or a combination of both phases. The minimization algorithm of Eq. (7) determines G of all such states and returns the state with the minimum G value. For example, for a single NaCl particle at low rh, Eq. (7) predicts a dry particle, the state with the minimum G, and continues to do so as rh increases. However, Eq. (7) eventually predicts the presence of water as rh reaches a critical value. At this point, Eq. (7) indicates G of a completely aqueous particle is lower than that of all other possible states. The rh at which this initially occurs is thus the DRH of the particle of interest. Similarly, for multicomponent particles, the DRH can be determined as the lowest rh at which Eq. (7) predicts the presence of water.

To predict the efflorescence behavior of aerosols, all possible aerosol components are "forced" to reside in the liquid phase by adding constraints to Eq. (7), eliminating the possibility of the formation of solid components. Doing so will allow the prediction of a supersaturated aqueous phase at rh below the DRH of all the aerosol components. Thermodynamically, this condition is described as metastable equilibrium. Mathematically, it corresponds to the addition of one constraint to Eq. (7), $n_s = 0$, where s corresponds to all solid components.

3.2. Comparison to equation-based approach

Many previous atmospheric aerosol models such as MARS, SEQUILIB, SCAPE, SCAPE2, and EQUISOLV attempt to solve the equilibrium problem in a different manner. The system is treated as a reactive one where specific reactions among the components of the system are assumed to occur, and an expression involving an equilibrium constant K is derived for each reaction (Pilinis and Seinfeld, 1987; Kim et al., 1993a). The resulting system of nonlinear algebraic equations is then solved with the solution of the system corresponding to a minimum of G. However, basing aerosol equilibrium calculations on a predetermined set of reactions introduces difficulties in predicting multistage behavior for volatile compounds. Consider for example the behavior of an NH_4NO_3–Na_2SO_4 mixed particle which can exist as a solid, liquid, or a combination of both phases. Fig. 3 shows the concentration of solid NH_4NO_3 for an NH_4NO_3–Na_2SO_4 particle ($\sim$6 wt% Na_2SO_4 initially) as a function of rh predicted by the equation-based approach of SCAPE2 and by the direct minimization method shown in Eq. (7). For this simulation only, both approaches include equivalent thermodynamic data (Wagman et al., 1982), both use the Kusik–Meissner method and Bromley method for determining binary and multicomponent activity coefficients respectively, and the ZSR relation for calculating a_w. For such a particle, the small amount of Na_2SO_4 deliquesces at a low rh causing the NH_4NO_3 fraction of the particle to gradually dissolve over a range of rh. The direct minimization solution predicts the gradual dissolution of NH_4NO_3 caused by the deliquescence of Na_2SO_4 whereas the equation-based approach of SCAPE2 predicts an instantaneous deliquescence of the entire particle at rh = 0.58; it cannot

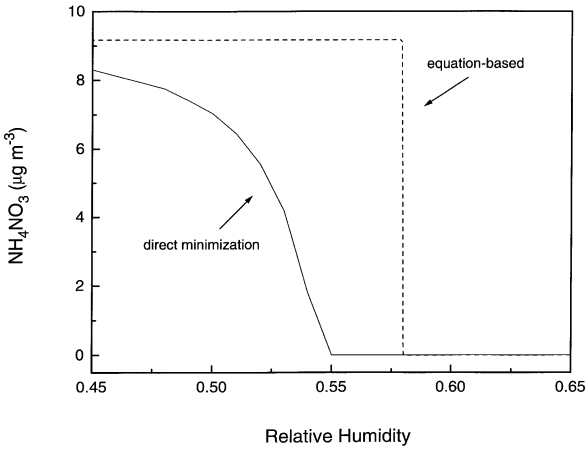

Fig. 3. Predicted concentration profile at 25°C of solid NH_4NO_3 by a direct minimization and by an equation based minimization of the Gibbs free energy for a mixed NH_4NO_3-Na_2SO_4 (~6 wt% Na_2SO_4 initially) particle. Total ammonia $= 10\,\mu g\,m^{-3}$, total nitrate $= 20\,\mu g\,m^{-3}$, and Na_2SO_4 $= 0.62\,\mu g\,m^{-3}$.

simulate the partial dissolution of NH_4NO_3 nor does it predict the deliquescence of Na_2SO_4 at low rh.

With an equation-based approach, the composition and state of the particle is predicted based on the following reactions and their corresponding equilibrium equations:

$$NH_3(g) + HNO_3(g) \rightleftarrows NH_4NO_3(s) \quad (8)$$

$$NH_3(g) + HNO_3(g) \rightleftarrows NH_4^+(aq) + NO_3^-(aq) \quad (9)$$

$$Na_2SO_4(s) \rightleftarrows 2Na^+(aq) + SO_4^{2-}(aq). \quad (10)$$

For the given system, the total ammonia, total nitrate, and total Na_2SO_4 concentrations are known and can be used to formulate three conservation of mass equations. The unknown variables are $NH_3(g)$, $HNO_3(g)$, $NH_4NO_3(s)$, $NH_4NO_3(aq)$, $Na_2SO_4(s)$, and $Na_2SO_4(aq)$, and hence, a system of six equations (three equilibrium relationships for Eqs. (8)–(10) and three for conservation of mass) can in principle be solved. However, Eqs. (8) and (9) both define expressions for the partial pressure product, $p_{NH_3}\, p_{HNO_3}$. If the particle consists of solid and aqueous NH_4NO_3, Eqs. (8) and (9) cannot be used simultaneously because they result in a set of inconsistent equations. Furthermore, for cases where only solid or liquid Na_2SO_4 is present, Eq. (10) does not hold; it holds for cases where both solid and liquid Na_2SO_4 are present. To circumvent the aforementioned difficulties with an equation-based approach, SCAPE2 assumes that only Eq. (8) or Eq. (9) describes the behavior of NH_4NO_3 and that Na_2SO_4 is solid at low rh. Doing so reduces the number of unknown variables and equations to three, and the potential inconsistency associated with Eqs. (8) and (9) is also eliminated. With such assumptions, the solution to the equation-based approach in this case is a local minimum of G of the system and not the global minimum; its G is higher than that of the global solution.

However, such assumptions, which are necessary to obtain a solution in an equation-based framework for simulating aerosol behavior, introduce errors in the prediction of multistage behavior for volatile compounds and in the deliquescence depression of salts in multicomponent systems as shown in Fig. 3. Aerosol behavior is a strong function of composition and as such, conditions suggesting multistage behavior and quantifying the degree of deliquescence depression are not known a priori. As such, modifying an equation-based algorithm to predict multistage behavior and deliquescence depression is difficult. A direct minimization of the Gibbs free energy such as that in Eq. (7) implicitly predicts multistage aerosol behavior and deliquescence depression without any a priori knowledge of the aerosol system behavior. For an equation-based approach, provided the equilibrium equations represent the actual behavior of the aerosol system, its solution corresponds to the global minimum of G and thus accurately reproduces aerosol behavior.

3.3. Assumptions of previous aerosol equilibrium models

Since computational efficiency is a primary objective of many equilibrium models, assumptions are made to simplify the equilibrium problem, predetermining to a certain extent the aerosol phases present. MARS, SEQUILIB, SCAPE, and SCAPE2 divide the entire rh and composition domains into several subdomains where only certain components are assumed to exist. Moreover, MARS and SEQUILIB assume that the DRH of individual components is independent of system composition. SCAPE, MARS, and SEQUILIB assume that the DRH is independent of temperature over the entire temperature range. AIM has been developed to model atmospheric aerosol behavior based on mass transfer and hence, will not be discussed further. MARS, SEQUILIB, SCAPE, and SCAPE2 have difficulties in predicting the composition dependence of the DRH of components in mixtures. For example, these models estimate a constant DRH for solutions containing a mixture of NH_4NO_3 and $(NH_4)_2SO_4$ regardless of the composition of the mixture. Potukuchi and Wexler (1995a, b) have shown that the DRH of multicomponent systems is composition dependent. Finally, only SCAPE2 has directly simulated aerosol efflorescence behavior to date.

4. Model evaluation

To determine the accuracy attainable with the current model, its predictions are compared with available

Table 2
Sensitivity of DRH to $\Delta G^0_{f(NH_4)_2SO_4}$ in GFEMN

$\Delta G^0_{f(NH_4)_2SO_4}$ (kJ mol^{-1})	% Deviation[b]	Predicted DRH $(NH_4)_2SO_4$ (%)
− 899.867	− 0.20	68.0
− 900.588	− 0.12	70.9
− 900.949	− 0.08	72.3
− 901.309	− 0.04	73.7
− 901.670	—	75.0
− 902.031	0.04	76.2
− 902.391	0.08	77.5
− 902.752	0.12	78.7
− 903.15[a]	0.16	79.9
− 903.473	0.20	80.9

[a]Value used in GFEMN.
[b]Deviation is percentage of adjusted value from orginial value.

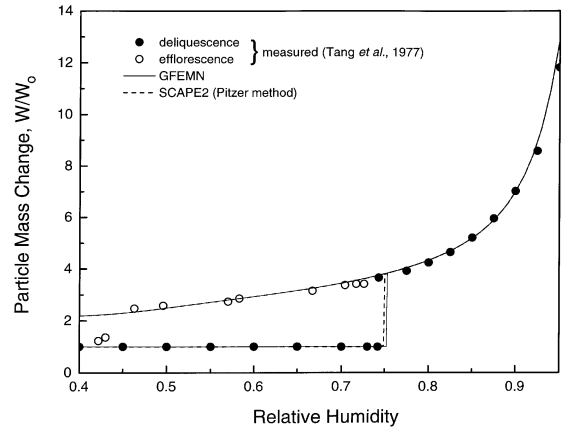

Fig. 4. Particle mass change for NaCl at 25°C as a function of relative humidity: model prediction versus observed results.

experimental results and those from SEQUILIB (single section version) and SCAPE2. Note that SEQUILIB and SCAPE2 are orders of magnitude faster than the current approach.

4.1. Single salts

All three models were first used to predict the behavior of $(NH_4)_2SO_4$ as a function of rh. Fig. 1 shows the experimentally observed growth of an $(NH_4)_2SO_4$ particle (Tang et al., 1981) along with growth profiles predicted from the Gibbs free energy minimization (GFEMN) model, SEQUILIB, and SCAPE2 at 25°C and 1 atm. GFEMN qualitatively predicts the sudden increase in size and the smooth deliquescence and efflorescence behavior of the particle. However, GFEMN underpredicts the DRH of $(NH_4)_2SO_4$ by 5%, and thus, a sensitivity analysis was performed to identify the cause of this behavior. The sensitivity of the deliquescence point to slight perturbations in $\Delta G^0_{f(NH_4)_2SO_4}$ in GFEMN is shown in Table 2. As shown, perturbations in $\Delta G^0_{f(NH_4)_2SO_4}$ of less than 0.5% cause a 5% shift in the predicted DRH of $(NH_4)_2SO_4$. The experimental uncertainty in $\Delta G^0_{f(NH_4)_2SO_4}$ is more than 0.5% and therefore, we elected to adjust $\Delta G^0_{f(NH_4)_2SO_4}$ from − 901.67 to − 903.15 kJ mol^{-1} to allow accurate prediction of experimentally observed DRH. Similar adjustments to ΔG^0_f are made for all aerosol salts (i.e. $(NH_4)_2SO_4$, Na_2SO_4, $NaNO_3$, NaCl). Table 1 shows the original values of ΔG^0_f in Wagman (1982), our adjusted values, the percent deviation of our adjusted values from the original values, and the measured DRH (Pilinis and Pandis, 1995) of each component. Adjusted values for ΔG^0_f will be used for all simulations. With the adjusted ΔG^0_f, GFEMN now reproduces within experimental error the DRH of $(NH_4)_2SO_4$ as seen in Fig. 1 (adjusted ΔG^0_f curve). As the particle grows on the deliquescence branch, GFEMN agrees with the measured results within 3% which is within experimental error. Along the efflorescence path, the discrepancy between predictions and measurements increases as rh decreases; at 80% rh, the discrepancy is 1.4% and at 53% rh, the discrepancy is approximately 20%.

The predictions of SCAPE2 and SEQUILIB also agree with the observed behavior of $(NH_4)_2SO_4$. SCAPE2 underpredicts the DRH by 10%, but since SCAPE2 was developed to predict the presence of water at rh lower than the DRH of all components, it encounters some difficulties in predicting DRH for some single salts. SEQUILIB correctly predicts the measured DRH, and above the DRH, the predictions of SCAPE2 and SEQUILIB are within 10% of the measured values. The prediction of SCAPE2 for the efflorescence behavior of $(NH_4)_2SO_4$ is similar to that of GFEMN. SEQUILIB cannot directly simulate aerosol efflorescence behavior. Tang et al. (1981) determined the crystallization point (30% rh) of $(NH_4)_2SO_4$, yet since GFEMN, SCAPE2, and SEQUILIB are based on thermodynamic equilibrium, they cannot reproduce crystallization points.

Fig. 4, depicting the behavior of a NaCl particle (Tang et al., 1977), further shows the ability of GFEMN to predict single salt behavior. At rh below 90%, GFEMN agrees within 1–2% with measured points on the deliquescence and efflorescence paths. Above 90% rh, the agreement is within approximately 10% of the measured results. The prediction of SCAPE2 is as accurate as that of GFEMN. SEQUILIB results are not included in Figure 4 since it was not developed to accurately model NaCl alone; it implicitly assumes that some sulfate is always present.

4.2. Binary salts

Atmospheric aerosols rarely consist of a single component. Fig. 5 shows model predicted behavior of

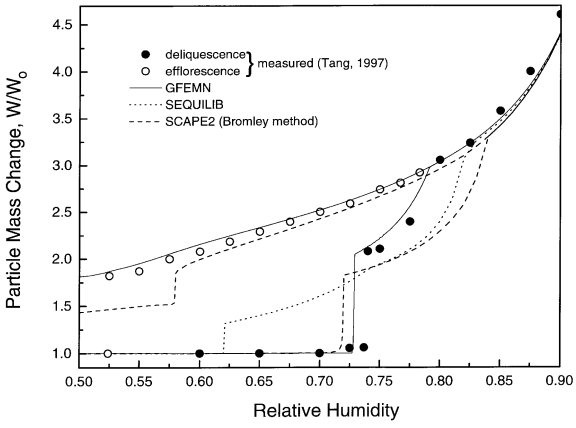

Fig. 5. Particle mass change at 25°C of a mixed Na_2SO_4–NaCl particle (equimolar mixture): model predictions versus observed results.

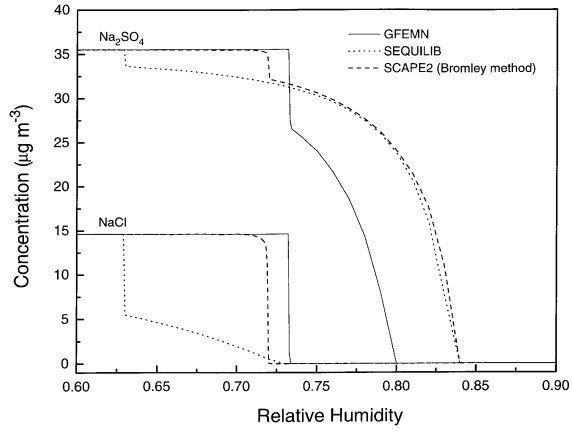

Fig. 6. Model predictions of component concentrations at 25°C for a mixed Na_2SO_4–NaCl (equimolar) particle.

a mixed NaCl–Na_2SO_4 particle against that observed by Tang (1997). For multicomponent systems, DRH depression and multistage growth patterns are observed. GFEMN predicts two stages of deliquescence; the first occurring from 73 to 79% rh and the second at 80% rh and above. In each stage and during efflorescence, it reproduces the measured behavior. The DRH prediction is in error by 1.4% indicating that a single adjustment of ΔG_f^o for solid components produces accurate DRH predictions for binary salt systems. Further discussion of adjusted parameters will be given at the end of the section. In the first stage (73–79% rh) of particle deliquescence, GFEMN is within 7% of the measured values. Over the second stage (80% rh and greater), the discrepancy increases from practically 0% to approximately 5% at 90% rh. During efflorescence, the predictions of GFEMN are within 5% of the measured values.

SCAPE2 and SEQUILIB also predict two stages of growth for the binary system. SCAPE2 slightly underpredicts the DRH and is within 25% of the measured values in the first deliquescence stage. In the second deliquescence stage, the error is 25% initially but then decreases to a value similar to that of GFEMN. Along the efflorescence path, SCAPE2 is accurate to within 5% except in the region below 58% rh. At 57% rh, SCAPE2 predicts a sudden decrease in the particle size resulting in a 20% error compared to observed efflorescence behavior. Below 58% rh, SCAPE2 assumes the water associated with the dissolution of Na_2SO_4 is negligible. Hence, below 58% rh, SCAPE2 will underpredict the water content of the system along the efflorescence branch for systems containing Na_2SO_4. SEQUILIB also predicts the multistage behavior of the NaCl–Na_2SO_4 particle, yet underpredicts the DRH by 12.1% which causes an error of up to 74% in predicting deliquescence below the measured DRH. Above the DRH in the first stage of deliquescence, the error in SEQUILIB's prediction reaches 20%, but then converges to the measured value as rh increases in the second deliquescence stage.

Fig. 6 shows the predicted behavior of the individual components of the NaCl–Na_2SO_4 system. Although no similar measurements are available, the results explain the discrepancies among the three models. Since NaCl has a lower DRH than Na_2SO_4, it deliquesces first and at a lower DRH than if it were to exist alone. The deliquescence of NaCl is accompanied by the gradual dissolution of Na_2SO_4 with its partitioning between the solid and aqueous phases determined by thermodynamic equilibrium. All three models reproduce this qualitative behavior, but do so in different regimes of rh. In addition to underpredicting the DRH of NaCl, SCAPE2 and SEQUILIB delay the dissolution of Na_2SO_4 which is the source of error in the second stage of deliquescence in Fig. 5. Since the predictions of GFEMN are the most accurate in predicting aerosol behavior based on Fig. 5, its component predictions are most probably an accurate representation of the system's behavior. However, as seen by the predictions of SCAPE2 and SEQUILIB, an equation-based solution can predict the gradual dissolution of some compounds.

Fig. 7, illustrating the behavior of a mixed NH_4NO_3–$(NH_4)_2SO_4$ particle (Tang et al., 1981), further evaluates the ability of the models to predict the behavior of binary systems. GFEMN is able to capture the multistage behavior observed as the particle dissolves. Below 90% total salt concentration, GFEMN predictions are within 2% of the measured a_w of the particle. SCAPE2 and SEQUILIB have significant difficulties in the 0.65–0.78 a_w range (very concentrated solutions), yet above 0.80, their predictions are in agreement with the measured values. Table 3 shows a comparison of experimentally determined DRH points (Tang, 1994b) of mixed

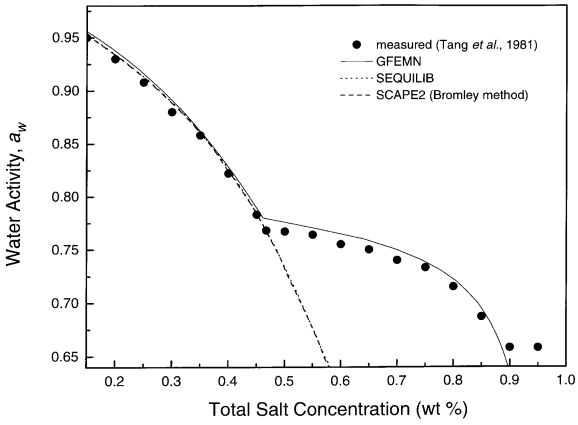

Fig. 7. Water activity as a function of total solute concentration at 25°C for an aqueous solution containing a mixed $(NH_4)_2SO_4$–NH_4NO_3 (82.6 wt%, 17.4 wt%, respectively) particle: model predictions versus observed results.

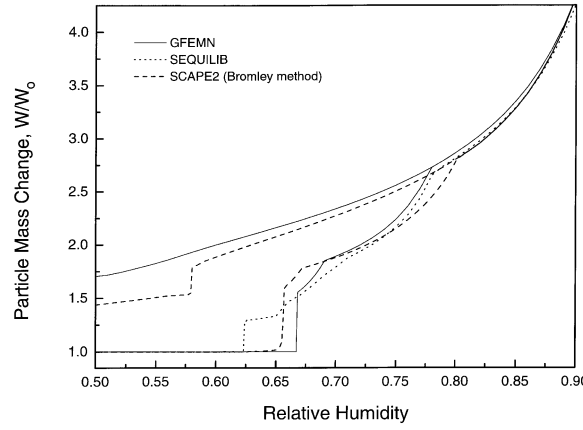

Fig. 8. Model predictions of the particle mass change at 25°C for a mixed Na_2SO_4–NaCl–$NaNO_3$ (equimolar) particle.

particles against those predicted by the three models and their resultant errors. The predictions of GFEMN and SCAPE2 are accurate.

Based on these results, a simple single adjustment in ΔG_f^0 for solid components results in accurate predictions of multicomponent aerosol behavior. As such, there is no need to adjust ΔG_f^0 for ions, gases, or other components. Furthermore, ΔG_f^0 is not dependent on aerosol or water composition and hence, adjustments in ΔG_f^0 will hold for all systems of interest regardless of composition; no curve fitting or any sort of external data fitting to experimental measurements is required. Adjustments in other variables such as activity coefficients and binary water activity data are less justified as these variables are strong functions of aerosol and water composition; a single adjustment for one condition will not hold for other conditions. Thus, a tedious examination of the entire aerosol composition and rh domains is required to make necessary fits to measurements of activity coefficients and binary water activities.

4.3. Multicomponent particles

Model predictions of a mixed, equimolar $NaNO_3$–NaCl–Na_2SO_4 particle are shown in Fig. 8. Although no reliable measurements are available for such systems, the $NaNO_3$–NaCl–Na_2SO_4 system can be viewed as adding $NaNO_3$ to the binary NaCl–Na_2SO_4 system in Fig. 5. Of the three components, $NaNO_3$ has the lowest DRH (74%) followed by NaCl (75%) and Na_2SO_4 (84%). Since there are three components in the mixture, a three-stage deliquescence process results. The first stage, beginning

Table 3
Deliquescence relative humidity (DRH) of mixed particles

Components	Measured DRH[a] (Tang, 1994b)	Predicted DRH					
		GFEMN	Error	SEQUILIB	Error	SCAPE2	Error
NaCl–$NaNO_3$	68.0 ± 0.4	67.6	0.4	62.1	5.9	67.3[b]	0.7
NaCl–Na_2SO_4	74.2 ± 0.3	72.8	1.4	62.1	12.1	72.0[b]	2.2
Na_2SO_4–$(NH_4)_2SO_4$	71.3 ± 0.4	70.2	1.1	80.1	8.7	67.5[c]	3.8
Na_2SO_4–$NaNO_3$	72.2 ± 0.2	72.2	0.0	62.1	10.1	72.8[c]	0.6
NaCl–$NaNO_3$	$71.0^{(at\ 9°C)}$	70.9	0.1	62.1	8.8	70.8[b]	0.2
NaCl–$NaNO_3$	$65.2^{(at\ 38°C)}$	65.5	0.3	62.1	3.4	64.5[b]	1.3
Na_2SO_4–$NaNO_3$	$75.3^{(at\ 10°C)}$	75.3	0.0	62.1	13.2	78.1[c]	2.8
Na_2SO_4–$NaNO_3$	$72.0^{(at\ 29°C)}$	71.5	0.5	62.1	9.4	69.9[b]	2.1

[a]25°C unless otherwise noted.
[b]Bromley method for activity coefficients.
[c]Pitzer method for activity coefficients.

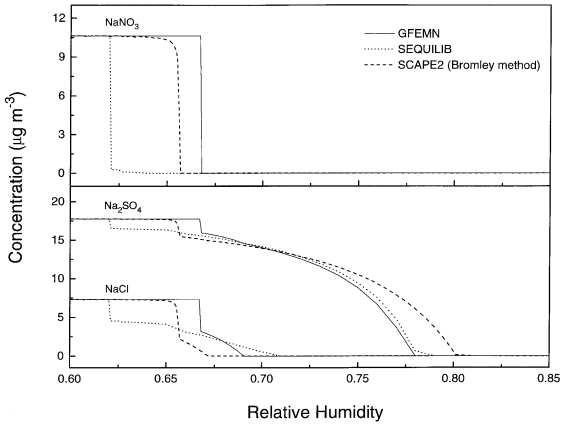

Fig. 9. Model predictions of component concentrations at 25°C for a mixed Na_2SO_4–NaCl–$NaNO_3$ (equimolar) particle.

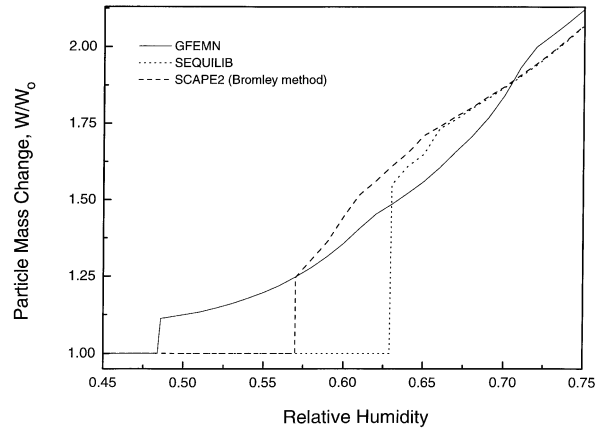

Fig. 10. Model predictions of the particle mass change at 25°C for a mixed NH_4NO_3–$NaNO_3$–Na_2SO_4 (equimolar) particle.

at a rh below that of the DRH of $NaNO_3$, consists of the deliquescence of $NaNO_3$, as it has the lowest DRH, and partial dissolution of NaCl and Na_2SO_4. The second stage shows the complete dissolution of the remaining solid NaCl and continued dissolution of Na_2SO_4. Finally, the third stage involves complete dissolution of the remaining solid Na_2SO_4, and only an aqueous phase is present. In each stage, the mixture grows by absorbing water as rh increases. Based on Fig. 8, GFEMN shows three discrete stages of deliquescence over the rh ranges: 66–69%, 69%–77%, and 77% and higher. SCAPE2 also shows three, separate growth stages with the first two stages starting at a lower rh than that of GFEMN. Compared to GFEMN, the predictions of SCAPE2 are within 13% in the first two stages of growth and during the third stage, its predictions are in agreement. Along the efflorescence path, the results of SCAPE2 are within 7% of the predictions by GFEMN, but as in the binary salt case, SCAPE2 predicts a sudden decrease in particle size at 58% rh which results in a discrepancy of approximately 20% at this rh range. The results of SEQUILIB agree with GFEMN and with SCAPE2 for rh $> 77\%$, yet since it underpredicts the DRH of the particle by 4%, SEQUILIB is within 45% of the prediction of GFEMN from 63% to 67% rh. From 67% to 77% rh, SEQUILIB is within 10% of the prediction by GFEMN. Fig. 9 shows the predicted behavior of the individual solid components of the mixture. Over the rh regime of 60–76%, SCAPE2 is generally within approximately 10% of GFEMN for Na_2SO_4, and although the discrepancy reaches 90% for NaCl at 66% rh, the large discrepancy is persistent over a small rh range (1–2%). In the rh range of 62%–66%, SEQUILIB underpredicts Na_2SO_4 but converges to the results of GFEMN within 1–2% at rh greater than 66%. For NaCl, SEQUILIB's discrepancy with GFEMN is as much as 64%, but this occurs over a small rh range (62–67%). Although no measured values are available for the behavior of such a system, all three models give similar results for the deliquescence and efflorescence behavior of the mixture.

In the previous system, all component DRHs were within a 10% rh range, 74–84%. Hence, differences in predictions of the three models show up over a small rh range. To further stress the models, three components with DRH spanning a larger range are examined. NH_4NO_3, $NaNO_3$, and Na_2SO_4 have a DRH of 62, 74, and 84%, respectively, spanning a rh range of 22%. Model predictions of the deliquescence behavior of the ternary system are shown in Fig. 10. A three-stage growth process results with the following behavior: the first stage involves deliquescence of NH_4NO_3 and the partial dissolution of $NaNO_3$ and Na_2SO_4, the second stage involves complete dissolution of the remaining $NaNO_3$ and continued dissolution of Na_2SO_4, and finally, the third stage consists of an aqueous solution of all three components absorbing water as rh increases. GFEMN reproduces this behavior showing three stages of growth: 48–62% rh, 62–72% rh, and 72% rh and above. SCAPE2 does not predict deliquescence until 57% rh which results in a 10–25% difference from that of GFEMN in the rh range 48–57%. From 57% rh to 72% rh, the difference between SCAPE2 and GFEMN ranges from 0 to 10% and above 72%, the difference in predictions is approximately 5%. SEQUILIB also underpredicts the DRH of the system by 15% resulting in a difference of 10–40% against the growth predicted by GFEMN in the rh range of 48–63%. From 63% rh to 70% rh, the difference is 0–8%, and above 70%, the difference is within 5%. Hence, unlike the former ternary system analyzed, significant differences between the model predictions for the present ternary system are evident over a broad rh range, from 48 to 72% rh.

4.4. Temperature dependence

Aerosol model predictions must be able to reflect behavior at temperatures other than 25°C. In considering the thermodynamics of aerosols, temperature-dependent variables include μ_i^0, γ_i, and $m_{io}(a_w)$. μ_i^0 is a function of temperature defined by Eq. (5), and thus its temperature dependence is easily accounted for in Eq. (7). For a specified solute concentration, the change in a_w from 20–25°C is generally less than 0.001 (Millero, 1979), and thus, although we are considering a broader temperature range, we assume that $m_{io}(a_w)$ does not change significantly. In addition, $m_{io}(a_w)$ for most atmospheric species of interest are available primarily at 25°C. Clegg et al. (1996) derived thermodynamic properties of aqueous $(NH_4)_2SO_4$ over a broad temperature range and showed that γ_i varies over the temperature range of 0–50°C by as much as 5%. The current activity coefficient model of Clegg et al. (1998) has been developed for 25°C, and therefore we implicitly assume that γ_i is independent of temperature. Hence, regarding the thermodynamic variables μ_i^0, γ_i, and $m_{io}(a_w)$, Eq. (7) includes the temperature dependence of μ_i^0 only, due to the limited availability of γ_i, and $m_{io}(a_w)$ over a broad temperature range. SCAPE2 and SEQUILIB also assume γ_i and $m_{io}(a_w)$ are temperature independent for similar reasons.

Tang and Munkelwitz (1993, 1994b) have conducted experiments and derived equations expressing the temperature dependence of the DRH of single and multicomponent aerosol particles. SCAPE2 incorporates DRH(T) for many salts based on the parameters determined by Wexler and Seinfeld (1991). Table 3 shows model DRH predictions and measurements by Tang and Munkelwitz for several binary systems at different temperatures. The predictions of all three models agree with measurements of Tang and Munkelwitz with the most accurate predictions given by GFEMN and SCAPE2. The agreement shows that GFEMN implicitly calculates the temperature dependence of deliquescence behavior without the use of any experimental data. SEQUILIB assumes the DRH of aerosols to be constant regardless of temperature resulting in inaccurate predictions of aerosol behavior near the DRH. Although the DRH temperature dependence would seem to depend on γ_i and $m_{io}(a_w)$ their dependence on temperature, assuming both to be constant does not introduce a significant source of error in predicting DRH(T) for the systems shown in Table 3. AIM (Wexler and Seinfeld, 1991), although it solves a different thermodynamic problem, can predict the DRH of single salts over a broad range of temperature.

5. Conclusions

Based on the results of the aerosol systems examined, the Gibbs free energy minimization approach presented here (GFEMN), which uses adjusted parameters for solid salts and the activity coefficient model of Clegg et al. (1998), accurately reproduces aerosol behavior for pure and binary aerosol systems over the entire rh range. This minimization approach requires no a priori knowledge other than the temperature, rh, and total concentrations (NH_3, HNO_3, HCl, H_2SO_4, Na) of the aerosol system to determine which components may be present or their respective concentrations and states. It implicitly determines a system's DRH regardless of temperature and composition allowing the accurate description of multistage growth patterns and DRH depression observed in the behavior of multicomponent systems. Assuming that only certain aerosol species exist in specific rh regimes often prevents accurate prediction of aerosol partitioning in certain ranges of rh of systems of higher complexity where DRH depression and multistage growth patterns are observed.

Moreover, GFEMN is able to predict the efflorescence behavior of aerosols and aerosol behavior over a range of temperatures. Aerosols are as probable to exhibit efflorescence as deliquescence behavior, and thus, accurately modeling both paths is essential. SCAPE2 is also able to simulate efflorescence behavior, and to accurately predict the behavior of aerosols over a range of temperatures. SEQUILIB does not attempt to predict aerosol efflorescence behavior during decreasing rh nor over a range of temperatures.

The use of adjusted thermodynamic parameters and the ZSR relation in GFEMN introduces slight inconsistencies with the activity coefficient model of Clegg et al. (1998). Clegg et al. (1998) developed an internally consistent thermodynamic model which calculates ion activity coefficients, water activity, and equilibrium constants. In spite of such inconsistencies, the combination of adjusted ΔG_i^0, the activity coefficient model of Clegg et al. (1998), and the ZSR relation allows the accurate calculation of the water activity and the reproduction of aerosol behavior. Models, like GFEMN, that do no rely on any a priori assumptions about the aerosol phase composition, appear, based on these limited tests, to reproduce well the phase transitions observed in laboratory experiments. Such tools can be used to improve the algorithms used for the description of phase transitions in equation-based models. Further evaluation of these models with laboratory aerosol data is necessary.

GFEMN does not attempt to predict the presence of any double salts such as $Na_2SO_4 \cdot 10H_2O$ and $3NH_4NO_3 \cdot (NH_4)_2SO_4$. Harrison and Sturges (1984) provide evidence of the existence of mixed sulfate-nitrate salts ($2NH_4NO_3 \cdot (NH_4)_2SO_4$), and Stelson and Seinfeld (1982c) show that for a mixed $NH_4NO_3/(NH_4)_2SO_4$ particle, the double salt $2NH_4NO_3 \cdot (NH_4)_2SO_4$ is present over a small rh range (0.63–0.66). Thus, the exclusion of double salts in GFEMN may result in minor errors in the prediction of aerosol behavior.

Furthermore, it should be noted that as GFEMN relies on a direct minimization of the Gibbs free energy, its minimization algorithm is computationally intensive making its use in large-scale transport models infeasible. SEQUILIB and SCAPE2 are computationally efficient making their incorporation into large-scale transport models worthwhile. Additionally, even if the present study focused on specific rh ranges where SEQUILIB and SCAPE2 encounter difficulties, their performance for the rest of the conditions is excellent.

Nonetheless, the results obtained from the current approach are encouraging as they show our current ability to reproduce the behavior of atmospheric aerosols based on thermodynamic principles, adjusted thermodynamic parameters, the activity coefficient model of Clegg et al. (1998), and experimental data. Although a direct minimization approach is computationally more demanding than solving a system of nonlinear equations, it has been shown to accurately reproduce atmospheric aerosol behavior. Based on the limited systems examined, GFEMN appears to more accurately reproduce aerosol behavior than SCAPE2 and GFEMN. However, as limited data on aerosol deliquescence behavior is available, there is a need for such experimental observations for ternary solids and more complicated systems over a wide range of temperatures to further determine the accuracy of model predictions. Our work provides indirect evidence for the need for very accurate measurements of the ΔG_f^0 of the solid aerosol components or equivalently of the corresponding dissociation constants.

Acknowledgements

The authors express their appreciation to Dr. Simon L. Clegg for use and instruction of his thermodynamic model, to Dr. Cristodoulos Pilinis for valuable discussions of the current work, and to two anonymous referees for their comments and suggestions. This research was conducted with support from the Environmental Protection Agency under grant R-824793010.

References

Bassett, M., Seinfeld, J.H., 1983. Atmospheric equilibrium model of sulfate and nitrate aerosols. Atmospheric Environment 17, 2237–2252.

Bromley, L.A., 1973. Thermodynamic properties of strong electrolytes in aqueous solutions. American Institute of Chemical Engineering Journal 19, 313–320.

Chan, C.K., Flagan, R.C., Seinfeld, J.H., 1992. Water activities of $NH_4NO_3/(NH_4)_2SO_4$ solutions. Atmospheric Environment A26, 1661–1673.

Chen, H., Sangster, J., Teng, T.T., Lenzi, F., 1973. A general method of predicting the water activity of ternary aqueous solutions from binary data. Canadian Journal of Chemical Engineering 51, 234–241.

Clegg, S.L., Pitzer, K.S., 1992a. Thermodynamics of multicomponent, miscible, ionic solutions: generalized equations for symmetrical electrolytes. Journal of Physical Chemistry 96, 3513–3520.

Clegg, S.L., Pitzer, K.S., Brimblecombe, P., 1992b. Thermodynamics of multicomponent, miscible, ionic solutions II. mixtures including unsymmetrical electrolytes. Journal Physics Chemistry 96, 9470–9479.

Clegg, S.L., Brimblecombe, P., 1994. A generalised multicomponent thermodynamic model applied to the $(NH_4)_2SO_4$-H_2SO_4-H_2O system to high supersaturation and low relative humidity at 298.15 K. Journal Aerosol Science 26, 19–38.

Clegg, S.L., Rard, J.A., Pitzer, K.S., 1994. Thermodynamic properties of a 0–6 mol kg^{-1} aqueous sulfuric-acid from 273.15 K to 328.15 K. Journal of Chemistry Society, Faraday Transactions 90, 1875–1894.

Clegg, S.L., Brimblecombe, P., 1995. Application of a multicomponent thermodynamic model to activities and thermal properties of 0–40 mol kg^{-1} aqueous sulfuric acid from < 200 to 328 K. Journal of Chemical Engineering Data 40, 43–64.

Clegg, S.L., Milioto, S., Palmer, D.A., 1996. Osmotic and activity coefficients of aqueous $(NH_4)_2SO_4$ as a function of temperature, and aqueous $(NH_4)_2SO_4$–H_2SO_4 mixtures at 298.15 K and 323.15 K. Journal of Chemical Engineering Data 41, 455–467.

Clegg, S.L., Brimblecombe, P., Wexler, A.S., 1998. A thermodynamic model of the system H^+–NH_4^+–Na^+–SO_4^{2-}–NO_3^-–Cl^-–H_2O at 298.15 K. Journal of Physical Chemistry 102, 2155–2171.

Cohen, M.D., Flagan, R.C., Seinfeld, J.H., 1987. Concentrated electrolyte solutions using the electrodynamic balance. 1. water activities for single-electrolyte solutions. Journal of Physical Chemistry 91, 4563–4574.

Denbigh, K., 1981. The Principles of Chemical Equilibrium, 4th ed. Cambridge University Press, Cambridge.

Hanel, G., Lehmann, M., 1981. Equilibrium size of aerosol particles and relative humidity: new experimental data from various aerosol types and their treatment for cloud physics application. Contributions to Atmospheric Physics 54, 57–71.

Harrison, R.M., Sturges, W.T., 1984. Physico-chemical speciation and transformation reactions of particulate atmospheric nitrogen and sulfur compounds. Atmospheric Environment 13, 1829–1833.

Hildemann, L.M., Russell, A.G., Cass, G.R., 1984. Ammonia and nitric acid concentrations in equilibrium with atmospheric aerosols: experiment vs. theory. Atmospheric Environment 9, 1737–1750.

Jacobson, M.Z., Tabazadeh, A., Turco, R.P., 1996. Simulating equilibrium within aerosols and nonequilibrium between gases and aerosols. Journal of Geophysical Research 101, 9079–9091.

Kim, Y.P., Seinfeld, J.H., Saxena, P., 1993a. Atmospheric gas-aerosol equilibrium I. Thermodynamic model. Aerosol Science and Technology 19, 157–181.

Kim, Y.P., Seinfeld, J.H., Saxena, P., 1993b. Atmospheric gas–aerosol equilibrium II. Analysis of common approximations and activity coefficient calculation methods. Aerosol Science Technology 19, 182–198.

Kusik, C.L., Meissner, H.P., 1978. Electrolyte activity coefficients in inorganic processing. American Institute of Chemical Engineering Symosium series, Symposium Series 173, 14–20.

Lurmann, F.W., Wexler, A.S., Pandis, S.N., Musarra, S., Kumar, N., Seinfeld, J.H., 1997. Modeling urban and regional aerosols: II. Applications to California's south coast air basin. Atmospheric Environment 31, 2695–2715.

Meng, Z., Seinfeld, J.H., Saxena, P., Kim, Y.P., 1995. Atmospheric gas-aerosol equilibrium: IV. Thermodynamics of carbonates. Aerosol Science and Technology 23, 131–154.

Meng, Z., Seinfeld, J.H., 1996. Time scales to achieve atmospheric gas-aerosol equilibrium for volatile species. Atmospheric Environment 30, 2889–2900.

Millero, F.J., 1979. In: Pytkowicz, R.M. (Ed.). Activity Coefficients in Electrolyte Solutions, vol. 2, CRC, Boca Raton, FL pp. 63–151.

Pilinis, C., Seinfeld, J.H., 1987. Continued development of a general equilibrium model for inorganic multicomponent atmospheric aerosols. Atmospheric Environment 21, 2453–2466.

Pilinis, C., Seinfeld, J.H., 1988. Development and evaluation of an eulerian photochemical gas-aerosol model. Atmospheric Environment 22, 1985–2001.

Pilinis, C., Pandis, S.N., 1995. Physical, chemical, and optical properties of atmospheric aerosols. In: The Handbook of Environmental Chemistry, vol. 4, Part D: Airborne Particulate Matter Springer-Berlin Heidelberg, New York.

Pitzer, K.S., 1986. Theoretical considerations of solubility with emphasis on mixed aqueous electrolytes. Pure and Applied Chemistry 58, 1599–1610.

Potukuchi, S., Wexler, A.S., 1995a. Identifying solid-aqueous phase transitions in atmospheric aerosols–I. Neutral-acidity solutions. Atmospheric Environment 29, 1663–1676.

Potukuchi, S., Wexler, A.S., 1995b. Identifying solid – aqueous phase transitions in atmospheric aerosols-II. Acidic solutions. Atmospheric Environment 29, 3357–3364.

Saxena, P., Hudischewskyj, A.B., Seigneur, C., Seinfeld, J.H., 1986. A comparative study of equilibrium approaches to the chemical characterization of secondary aerosols. Atmospheric Environment 20, 1471–1483.

Stelson, A.W., Seinfeld, J.H., 1982a. Relative humidity and temperature dependence of the ammonium nitrate dissociation constant. Atmospheric Environment 16, 983–992.

Stelson, A.W., Seinfeld, J.H., 1982b. Relative humidity and pH dependence of the vapor pressure of ammonium nitrate-nitric acid solutions at 25°C. Atmospheric Environment 16, 993–1000.

Stelson, A.W., Seinfeld, J.H., 1982c. Thermodynamic prediction of the water activity, NH_4NO_3 dissociation constant, density, and refractive index for the NH_4NO_3–$(NH_4)_2SO_4$–H_2O system at 25°C. Atmospheric Environment 16, 2507–2514.

Tang, I.N., 1997. Thermodynamic and optical properties of mixed-salt aerosols of atmospheric importance. Journal of Geophysical Research 102, 1883–1893.

Tang, I.N., Munkelwitz, H.R., Davis, J.G., 1977. Aerosol growth studies – II. Preparation and growth measurements of monodisperse salt aerosols. Journal of Aerosol Science 8, 149–159.

Tang, I.N., Munkelwitz, H.R., 1986. The growth and nucleation of hygroscopic aerosols. In: Aerosols: Formation and Reactivity, Proc. 2nd Int. Aerosol Conf., Berlin, 22–26, September 1986. Pergamon Press, Oxford.

Tang, I.N., Munkelwitz, H.R., 1993. Composition and temperature dependence of the deliquescence properties of hygroscopic aerosols. Atmospheric Environment 27A, 467–473.

Tang, I.N., Munkelwitz, H.R., 1994a. Water activities, densities, and refractive indices of aqueous sulfates and sodium nitrate droplets of atmospheric importance. Journal of Geophysical Research 99, 18 801–18 808.

Tang, I.N., Munkelwitz, H.R., 1994b. Aerosol phase transformation and growth in the atmosphere. Journal of Applied Meteorology 33, 791–797.

Tang, I.N., Wong, W.T., Munkelwitz, H.R., 1981. The relative importance of atmospheric sulfates and nitrates in visibility reduction. Atmospheric Environment 12, 2463–2471.

Wagman, D.D., Evans, W.H., Parker, V.B., Harlow, I., Baily, S. M., Schumm, R.H., 1968. Selected values of chemical thermodynamic properties; tables for the first thirty-four elements in the standard order of arrangement. NBS Technical note 270–273.

Wexler, A.S., Seinfeld, J.H., 1990. The distribution of ammonium salts among a size and composition dispersed aerosol. Atmospheric Environment 24A, 1231–1246.

Wexler, A.S., Seinfeld, J.H., 1991. Second-generation inorganic aerosol model. Atmospheric Environment 25A, 2731–2748.

Winkler, P., 1986. The growth of atmospheric aerosol particles with relative humidity. Physica Scripta 37, 223–230.